Solar Energy Vol. 39, No. 6, pp. 499–512, 1987
Printed in the U.S.A.

0038-092X/87 $3.00 + .00

LOSS-OF-LOAD PROBABILITIES FOR STAND-ALONE PHOTOVOLTAIC SYSTEMS

S. A. KLEIN and W. A. BECKMAN
Solar Energy Laboratory, University of Wisconsin-Madison

Abstract—A general method is presented for estimating the loss-of-load probability (LLP) of stand-alone photovoltaic systems. The method was developed by correlating simulation results. The simulations were driven with synthetic radiation sequences having the same statistical significance as available historical data. The method assumes a constant nighttime load and accounts for the distribution and persistence in daily solar radiation data. It is shown that the 10-year average performance of systems having loss-of-load probabilities less than about .01 can vary greatly from one 10-year period to the next and thereby cannot be considered realistic performance estimates of a system during its lifetime.

1. DAILY SOLAR RADIATION DISTRIBUTION AND PERSISTENCE

The general concern of this work is the effect of daily solar radiation distribution and persistence on the loss-of-load probability of stand-alone photovoltaic systems.

The distribution of daily solar radiation refers to the relative numbers of poor, average, and excellent days of sunshine which together compose the long-term average. Liu and Jordan[1] were first to note that the distribution can be represented in a location-independent manner by defining the clearness index, K, to be the ratio of daily to extraterrestrial radiation and relating the distribution of K values to $\overline{K}$, the long-term monthly average clearness index. Bendt et al.[2] and Hollands and Huget[3] have developed analytic forms for the cumulative distributions that are in excellent agreement with each other and with the original Liu–Jordan distributions. The distribution of solar radiation has been shown to have a significant effect on the performance of many different types of thermal and photovoltaic solar energy systems[4–9].

The persistence of solar radiation refers to the dependence of today's solar radiation on the solar radiation of preceding days. Persistence of daily solar radiation has been studied by Klein[10], Brinkworth[11], Bartoli et al.[12], and Graham[13]. All these authors concluded that the persistence in daily solar radiation can be adequately described by a first order autoregressive process. The single parameter of this model is the correlation coefficient between the daily solar radiation on successive days defined by

$$\phi = \frac{\sum^{n-1} (H_t - \overline{H})(H_{t+1} - \overline{H})}{\sum^{n-1} (H_t - \overline{H})^2} \qquad (1)$$

where H_t and H_{t+1} are the daily solar radiation per unit area on a surface for days t and $t + 1$, and $\overline{H}$ is the average daily radiation during a period of n days. Agreement is observed in the annual average values of ϕ for diverse locations and climates as seen in Table 1. Most of the annual values of ϕ range between 0.2 and 0.3 with a few values as low as 0.15 or as high as 0.4. This observation is also true on a monthly basis as shown in Table 2. The ϕ values reported in Table 2 were calculated as the average of individual monthly values for 23 (or 24) years of SOLMET[14] data. This table shows that ϕ has some seasonal dependence (as noted by others) and, furthermore, that it is highly variable from one year to the next, as indicated by the large standard deviations of the monthly values.

The values of ϕ seen in Tables 1 and 2 are relatively small and they exhibit large year-to-year variability, implying that today's daily solar radiation is only weakly related to yesterday's. (The persistence of daily average ambient temperatures is much stronger with average correlation coefficients of about 0.7.) Ordinarily, the weak persistence has a small effect on the performance of solar energy systems. However, the effects of both solar radiation distribution and persistence become increasingly important as the fraction of the load to be supplied by the solar system reaches high values. This increased sensitivity occurs because the storage unit is more often full or nearly full and less able to buffer the effects of varying conditions. Persistence always has a negative effect on system performance. A series of days with low radiation levels causes the storage unit to become depleted, whereas energy may have to be dumped during a series of days with high radiation. Radiation distribution and persistence have a significant impact on the design of a stand-alone photovoltaic system designed to have a high level of reliability.

2. EXISTING METHODS FOR ESTIMATING LOSS-OF-LOAD PROBABILITY

The loss-of-load probability (LLP) is defined here as the long-term monthly average fraction of

Table 1. Annual value of ϕ for various locations

Location	Latitude	Years	ϕ	Source
Bracknell, England	51.4	7	0.21	[11]
Alghero, Italy	40.6	3	0.19	[12]
Amendola, Italy	41.5	3	0.24	[12]
Ancona, Italy	43.6	3	0.24	[12]
Brindisi, Italy	40.6	3	0.20	[12]
Capo Mele, Italy	43.9	3	0.22	[12]
Capo Palinur, Italy	40.0	3	0.20	[12]
Crotone, Italy	39.1	3	0.24	[12]
Gela, Italy	37.1	3	0.17	[12]
Messina, Italy	38.2	3	0.25	[12]
Milano, Italy	45.4	3	0.31	[12]
Monte Cimone, Italy	44.2	3	0.38	[12]
Olbia, Italy	40.9	3	0.21	[12]
Pantelleria, Italy	36.8	3	0.24	[12]
Pescara, Italy	42.4	3	0.32	[12]
Pian Rosa, Italy	42.4	3	0.23	[12]
Pianosa, Italy	42.6	3	0.16	[12]
Pisa, Italy	43.7	3	0.31	[12]
Rome, Italy	41.8	3	0.30	[12]
Denver, Colorado	39.7	13	0.25	[25]
Toronto, Ontario, Canada	43.7	10	0.25	[13]
Swift Current, SAS, Canada	50.3	10	0.27	[13]
Vancouver, BC, Canada	49.0	10	0.35	[13]
Madison, WI	43.1	23	0.22	[14]
Albuquerque, NM	35.0	23	0.29	[14]
Seattle, WA	47.5	23	0.24	[14]
New York, NY	40.8	23	0.16	[14]
Columbia, MO	39.0	23	0.22	[14]

the load that is not supplied by a stand-alone photovoltaic system. This index has also been referred to as the probability of loss of power, 1—the long-term availability (or reliability), the expected value of the daily energy deficit, and the long-term average auxiliary fraction.

Methods for selecting array and battery sizes so as to obtain a specified loss-of-load probability have been developed by Bucciarelli[15, 16], Chapman[17], and Gordon[18]. Bucciarelli[15] presents an analytical model for the loss-of-load probability derived by approximating the probability density function of the difference between the daily array output and the load with two events and by assuming the daily storage charge/discharge process can be represented as a one-step Markov process. In this model, the daily load is assumed to be constant and presumably, uniformly distributed over 24 hours. The inputs to this model are the long-term average and standard deviation of the array output. Bucciarelli's model neglects the effects of persistence although he notes that "any appreciable correlation in weather will significantly alter (the) results." In a later paper, Bucciarelli[16] presented an extended method that considered persistence and requires ϕ as an additional input. Gordon[18] shows that the problem of designing a photovoltaic system to have a specified loss-of-load probability

Table 2. Average and monthly standard deviations of ϕ (based on 23.5 years of SOLMET data)

Month	Madison WI	Albuquerque NM	Seattle WA	New York NY	Columbia MO
Jan	0.209/.176	0.254/.197	0.205/.281	0.034/.184	0.219/.180
Feb	0.219/.183	0.305/.154	0.243/.228	0.120/.217	0.219/.208
Mar	0.258/.205	0.261/.162	0.229/.216	0.184/.159	0.220/.150
Apr	0.197/.160	0.272/.179	0.260/.167	0.142/.171	0.124/.185
May	0.233/.157	0.219/.181	0.201/.154	0.128/.205	0.194/.180
Jun	0.174/.228	0.251/.199	0.198/.127	0.206/.162	0.235/.220
Jul	0.126/.134	0.230/.148	0.298/.192	0.157/.199	0.124/.173
Aug	0.167/.177	0.292/.170	0.236/.195	0.165/.226	0.205/.196
Sep	0.246/.191	0.339/.295	0.331/.167	0.267/.164	0.275/.173
Oct	0.420/.177	0.482/.209	0.263/.199	0.252/.192	0.357/.163
Nov	0.234/.212	0.302/.222	0.266/.173	0.125/.168	0.227/.220
Dec	0.195/.169	0.260/.146	0.206/.128	0.099/.213	0.252/.151

is analogous to problems in other disciplines (such as water management), for which analytical solutions have been developed. He describes a method similar to that of Bucciarelli[16] using a three-event representation of the array output minus load probability density function. Gordon also assumes a constant daily load evenly distributed over 24 hours but notes that his model can be used for nighttime loads by adding one load-day of storage to the actual storage capacity of the system.

The methods of Bucciarelli and Gordon have several limitations. They both require the standard deviation of the daily array output as an input, but neither author indicates how this parameter is to be obtained when years of historical data are not available. The random walk process on which the methods are based assumes that the daily array output is a normally distributed variable. However, the probability density function of daily solar radiation, which strongly depends on $\overline{K}$, can be quite skewed. As the ratio of the average array output to the average daily load is increased, both methods reach a point (within the range of practical design interest) in which the analytic equations are no longer applicable and yield meaningless results. Neither author compares the results of his model with simulation results. Finally, the methods do not provide any information on the variability associated with a specified LLP. It is shown here that 10-year averages of the auxiliary fraction have a large variability for LLP values less than about .01 and periods of hundreds of years may be required to realize their designed performance level.

Chapman[17] used a daily simulation model driven by 24 years of SOLMET data from 18 sites to calculate the availability (i.e., the annual fraction of the load supplied by solar energy) of stand-alone photovoltaic systems. The model is a daily energy balance on the battery with a constant daily load uniformly distributed over 24 hours. He shows that for the same values of the ratios of array output and battery capacity to the load, the availability of a system varies significantly with location. The reason for this variation is shown here to be primarily a result of the differing radiation distributions in these locations. Chapman shows that the location dependence of the results can be reduced by correlating the collector array design insolation to the typical worst month daily insolation. He further presents distributions of the yearly availability that show large year-to-year variability and a bimodal shape with a sharp peak at 0.9999. Chapman's availabilities are presented on an annual basis, which results in higher availabilities (and less variability) for the same system characteristics than the monthly average results of Bucciarelli and Gordon, and the results presented here. Chapman's long-term average values of (1—availability) are only an estimate of the loss-of-load probability values as they are based on 24 years of data; an equally probable—but different—24-year weather sequence can result in significantly different availability values.

3. DESCRIPTION OF THE SIMULATION MODEL

Simulation models of stand-alone photovoltaic systems were constructed with both hourly and daily time steps for nighttime and uniform load distributions. All models assume the energy output of the photovoltaic array to flow through the battery and the system efficiency to be constant for monthly periods, as assumed by Bucciarelli, Gordon, and Chapman. The validity of a constant system efficiency is supported by the results of Ambrosone et al.[19], who have found monthly solar fractions calculated using daily timesteps and constant system efficiency to be in good agreement with detailed models with efficiency calculated on an hourly basis, particularly for battery storage capacities greater than twice the average daily load. The model used to generate the loss-of-load probability figures in Section 5 is similar to that used by Chapman, but differs in that a 24-hour period is broken into day-and-night periods and the load is assumed to occur during the night.

An energy balance on the battery during the daytime period is

$$B_d = \text{MIN}(B_n + \text{SLR}, B_{\max}) \tag{2}$$

where B_d and B_n are the ratios of the recoverable energy in the battery divided by L, the effective daily load (i.e., the daily load divided by the average inverter efficiency) at the end of the daytime and nighttime periods, respectively. L is taken to be a constant. $B_{\max}$ is the ratio of the maximum usable capacity of the battery to the effective load. SLR, the solar-to-load ratio, is defined as

$$\text{SLR} = \frac{A\overline{H}\eta}{L} \tag{3}$$

where A is the array area, $\overline{H}$ is the monthly average daily total solar radiation per unit area incident on the plane of the array, and η is an overall system efficiency. η is the product of efficiencies of the array, the power conditioning equipment, and the battery charge and discharge efficiencies.

An energy balance on the battery during the nighttime period results in

$$B_n = B_d - 1 \tag{4}$$

Negative battery charges are not allowed. If B_n is calculated to be less than zero, a dimensionless energy deficit is incremented by $-B_n$ and B_n is then set to zero. The dimensionless energy deficit is the auxiliary fraction, AUX. If the calculations are done over a sufficiently long period to fully characterize the statistical nature of the solar radiation,

Table 3. Simulation results for January in Madison, WI

SLR	B_{max}	(a) AUX fraction Night load Daytime step	(b) AUX fraction 24-hour load Daytime step	(c) AUX fraction 24-hour load Hour time step
0.8	1	2.629E-01	2.058E-01	2.237E-01
1.2	1	1.526E-01	4.862E-02	9.617E-02
1.6	1	9.764E-02	1.894E-02	5.394E-02
2.0	1	6.589E-02	8.113E-03	3.170E-02
0.8	2	2.056E-01	1.975E-01	2.005E-01
1.2	2	4.862E-02	1.839E-02	3.498E-02
1.6	2	1.894E-02	2.833E-03	1.108E-02
2.0	2	8.113E-03	3.412E-04	3.670E-03
0.8	3	1.973E-01	1.958E-01	1.960E-01
1.2	3	1.839E-02	8.769E-03	1.240E-02
1.4	3	7.550E-03	2.241E-03	4.969E-03
1.6	3	2.833E-03	0.0	1.383E-03
2.0	3	3.412E-04	0.0	0.0

the AUX is the loss-of-load probability, LLP. Since the simulations are run for long time periods, the initial state of the battery has no effect.

Simulation results for a range of values of SLR and B_{max} based on 24 years of horizontal SOLMET data for January in Madison, WI are shown in Table 3. Column (a) lists the results obtained using the simulation model described above. Identical results were obtained using the hour-by-hour model with a nighttime load distribution. The results in column (b) were obtained using a simulation model with daily timesteps and a 24-hour uniform load distribution, as assumed in the models of Bucciarelli, Gordon, and Chapman. The results in column (c) also assume a 24-hour load distribution but were obtained from an hour-by-hour analysis.

As expected, the auxiliary fractions calculated in column (c), assuming a uniform load distribution, are lower than those obtained in column (a), assuming a nighttime load. The daily time step-uniform load model, column (b), unavoidably assumes that the solar radiation is uniformly distributed over a 24-hour period and results in significantly lower auxiliary fractions than observed for the hour-by-hour results in column (c). As Gordon noted, the simulation results in column (b) are exactly (to three significant figures) equal to the results of column (a) if B_{max} is reduced by 1. Similar results were observed for other months and locations.

4. STATISTICAL GENERATION OF DAILY SOLAR RADIATION

The use of historical solar radiation data has several disadvantages when used to drive simulations designed to calculate the loss-of-load probability. Most importantly, even 20 years of data are insufficient to obtain accurate estimates of LLP for LLP values less than about .01, as seen in Section 5. Second, the effects of radiation distribution and persistence on LLP cannot be independently investigated. These problems are eliminated by using synthetic solar radiation data.

Synthetic values of K, were generated using a method developed by Graham[13]. Graham models the persistence in a series of K values with an autoregressive model of order 1. However, rather than work with the K values themselves, which are bounded and have a skewed distribution, Graham transforms the K values into a series with a Gaussian distribution having a mean of 0 and a variance of 1. The transformation uses the probability distribution of daily K values, thereby ensuring that the synthetic data have the correct statistical distribution. The Hollands–Huget analytical form of the probability distribution was used in our study, although the relation of Bendt et al. could also have been used.

Graham's method requires as input data, $\overline{K}$, K_{max}, and ϕ. Hollands and Huget recommend that K_{max} be a constant equal to 0.864. Their probability distribution assumes K_{min} to be 0.0. A slight modification was made so that values of K calculated to be less than 0.03 were set to 0.03 based on observations of K_{min} values for five U.S. locations. Table 4 compares 23-year (700-day) statistics of historical daily solar radiation data for selected months and locations with those of synthetic data. The synthetic data were generated in two ways: (1) using historical values of K_{min} and K_{max} and (2) setting K_{min} and K_{max} to constants equal to 0.03 and 0.864, respectively. Both sets of synthetic data closely reproduce the historical statistics in all respects. Differences in the historical and synthesized values of ϕ in Table 4 can be observed, as, for example, May in Madison. However, there is a relatively large standard deviation associated with the 23-year average values (approximately equal to $\sigma_\phi/\sqrt{23}$) and the differences are consistent with the expected variation. Figure 1 shows that the historical (dotted lines) and synthetic (with constant K_{min} and K_{max}, solid lines) probability distributions for January in

Table 4. Comparison of historical and synthetic daily radiation statistics

	$\overline{K}$	σ_{K^-}	K_{min}	K_{max}	σ_K	ϕ	σ_ϕ
Madison: January							
Historical	0.441	0.047	0.029	0.838	0.199	0.209	0.177
Synthetic (1)	0.447	0.037	0.031	0.827	0.207	0.214	0.170
Synthetic (2)	0.447	0.039	0.032	0.852	0.215	0.214	0.172
Madison: March							
Historical	0.500	0.050	0.037	0.917	0.227	0.258	0.205
Synthetic (1)	0.507	0.050	0.039	0.908	0.224	0.267	0.155
Synthetic (2)	0.506	0.046	0.032	0.858	0.205	0.264	0.156
Madison: May							
Historical	0.506	0.058	0.042	0.809	0.201	0.233	0.157
Synthetic (1)	0.509	0.024	0.044	0.801	0.179	0.144	0.179
Synthetic (2)	0.508	0.027	0.032	0.855	0.201	0.147	0.176
Albuquerque: August							
Historical	0.702	0.032	0.130	0.867	0.108	0.292	0.170
Synthetic (1)	0.699	0.027	0.165	0.862	0.112	0.210	0.179
Synthetic (2)	0.699	0.027	0.174	0.858	0.110	0.210	0.179
Seattle: January							
Historical	0.308	0.061	0.018	0.960	0.208	0.205	0.281
Synthetic (1)	0.304	0.034	0.021	0.920	0.227	0.173	0.153
Synthetic (2)	0.304	0.033	0.032	0.831	0.212	0.177	0.157
Seattle: December							
Historical	0.300	0.036	0.012	0.772	0.206	0.206	0.128
Synthetic (1)	0.295	0.036	0.014	0.764	0.187	0.180	0.158
Synthetic (2)	0.295	0.039	0.032	0.851	0.201	0.171	0.162
New York: February							
Historical	0.410	0.039	0.003	0.855	0.211	0.034	0.184
Synthetic (1)	0.410	0.046	0.005	0.818	0.214	0.045	0.179
Synthetic (2)	0.410	0.048	0.032	0.844	0.220	0.045	0.178
Columbia: July							
Historical	0.596	0.043	0.078	0.806	0.147	0.124	0.173
Synthetic (1)	0.611	0.031	0.033	0.797	0.138	0.056	0.172
Synthetic (2)	0.615	0.038	0.032	0.852	0.169	0.060	0.174

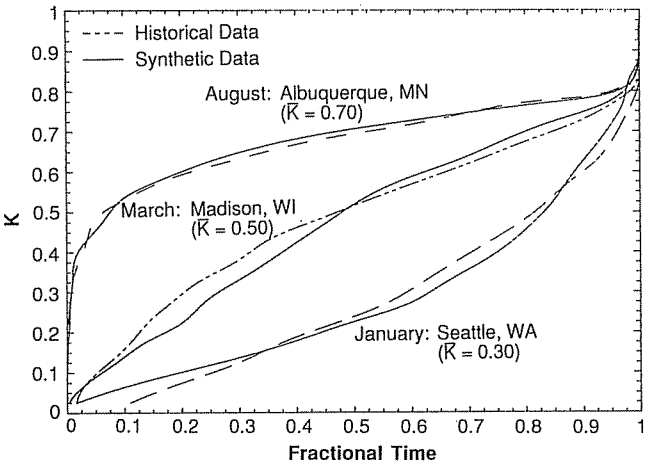

Fig. 1. Comparison of synthetic (solid lines) and historical (dotted lines) cumulative probability distributions for January in Seattle, WA, March in Madison, WI, and August in Albuquerque, NM.

Seattle ($\overline{K} = 0.30$), March in Madison ($\overline{K} = 0.50$), and August in Albuquerque ($\overline{K} = 0.70$) agree to within the standard deviations reported by Bendt et al. Both the historical and synthetic distributions based on 23 years of data exhibit some waviness not present in the Holland–Huget analytical distribution. The constant values of K_{min} and K_{max} were used in all following work.

5. LOSS-OF-LOAD PROBABILITIES

Graham's radiation model synthesizes sequences of daily values of K with the same statistical properties as observed in the historical data. The simulation model described in Section 3 can use either SOLMET or synthetic radiation data. The advantage of the synthetic data for the purpose at hand is that the effects of radiation distribution (through $\overline{K}$ and ϕ) can be studied independently and radiation sequences representative of a specified month can contain any number of days.

The number of days of operation needed for a system to realize its loss-of-load probability has not been addressed in previous studies. The effect of number of days can be seen in Fig. 2 where auxiliary fractions for $B_{max} = 4$, $\overline{K} = 0.5$, and $\phi = 0.30$ simulated using 300, 1500, 3000, and 30,000 days (i.e., 10, 50, 100, and 1000 years) of synthetic radiation data have been plotted. Significant differences in the calculated auxiliary fractions at a particular value of SLR are observed for auxiliary fractions less that about 0.01; these differences tend to increase as the auxiliary fraction approaches zero. Different, but equally probable, sets of synthetic data can be generated by changing the seed value used for the random number generator. Quite different-looking curves are obtained for the 300- and 1500-day results by choosing different random number sequences. Presumably, simulation results using different 20-year periods of historical data would also produce different curves if such data were available, implying that the 24 years of SOLMET data are insufficient to allow accurate estimates of low LLP values.

As expected, the simulation results converge to a unique auxiliary fraction at each SLR value as the number of days is increased; the number of days needed to obtain convergence is, however, surprisingly large. Differences are still observed between the results obtained using 3000 and 30,000 days of data for auxiliary fractions less than 0.01. Using 30,000 days of data produces a smooth curve that is not affected by the seed value used for the random number generator. All following results were obtained using 30,000 days of synthetic radiation data. The auxiliary fractions calculated with 30,000 days of data are assumed to be identical to the loss-of-load probabilities.

Figure 3 illustrates the effect of persistence on the loss-of-load probability. The solid lines were generated assuming that there is no persistence in the daily solar radiation (i.e., $\phi = 0$). The dotted lines correspond to $\phi = 0.45$, the maximum persistence observed in any location. For a given system configuration, the LLP is lower when there is no persistence, for reasons given in Section 1. However, persistence has no effect on the results for $B_{max} = 1$ for the nighttime load distribution considered. In this case, the battery is in a fully discharged state at the beginning of every day and the solar radiation occurring on previous days has no effect.

The persistence in daily solar radiation can be characterized, somewhat conservatively in most cases, with $\phi = 0.3$. Figures 4 through 10 present loss-of-load probabilities for $\phi = 0.3$ and $\overline{K}$ values between 0.1 and 0.7. A comparison of these figures shows a marked effect of radiation distribution on the loss-of-load probability. For the same values of SLR and B_{max}, LLP is always larger when there is more variability in the daily solar radiation. Increased variability results in a higher occurrence of

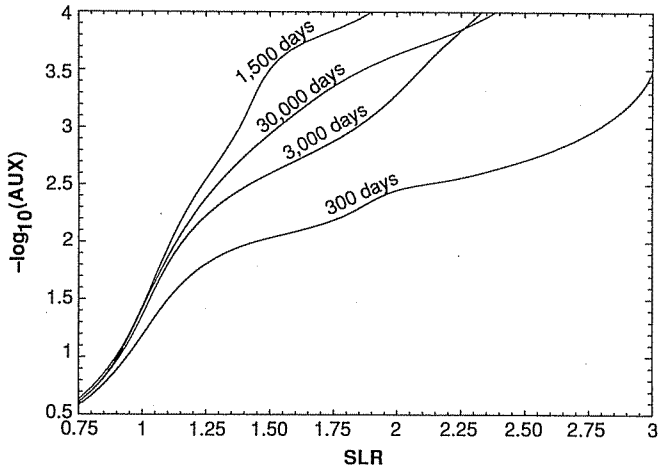

Fig. 2. Effect of number of days of data on the calculated auxiliary fraction for $\overline{K} = 0.5$, $B_{max} = 4$, and $\phi = 0.3$.

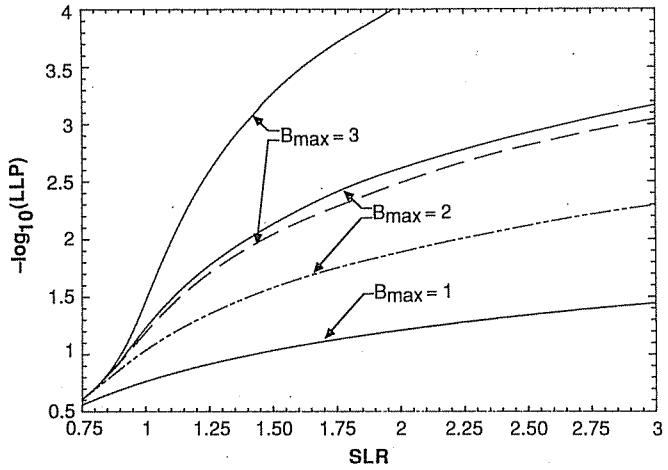

Fig. 3. Loss-of-load probabilities vs SLR for B_{max} of 1, 2, and 3 with $\overline{K} = 0.5$ and $\phi = 0$ (solid lines) and $\phi = 0.45$ (dotted lines).

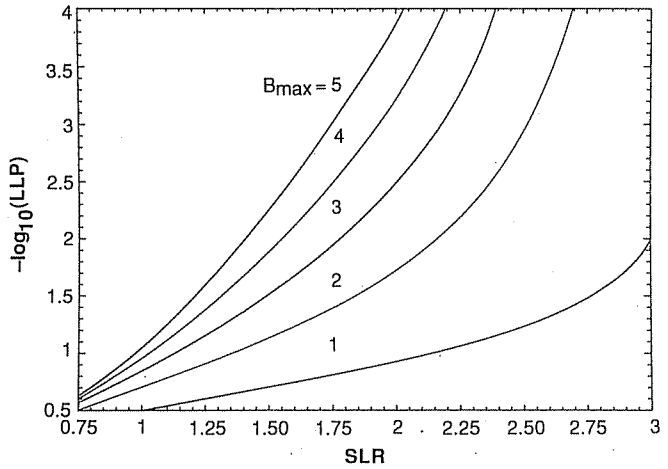

Fig. 4. Loss-of-load probabilities vs SLR for $\phi = 0.30$ and B_{max} between 1 and 5 for $\overline{K} = 0.1$ ($\sigma_H/\overline{H} = 0.935$).

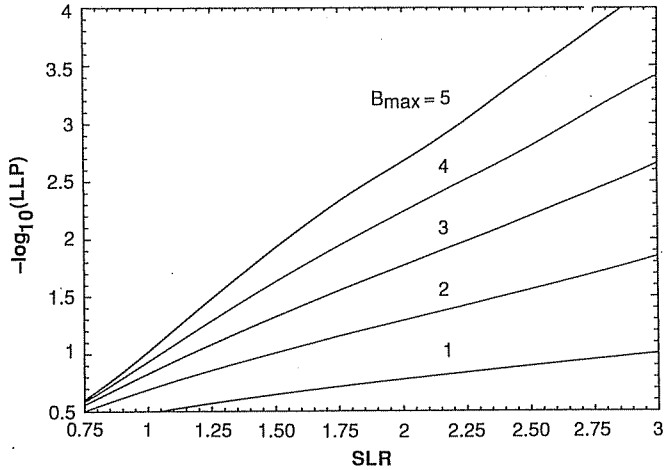

Fig. 5. Loss-of-load probabilities vs SLR for $\phi = 0.30$ and B_{max} between 1 and 5 for $\overline{K} = 0.2$ ($\sigma_H/\overline{H} = 0.834$).

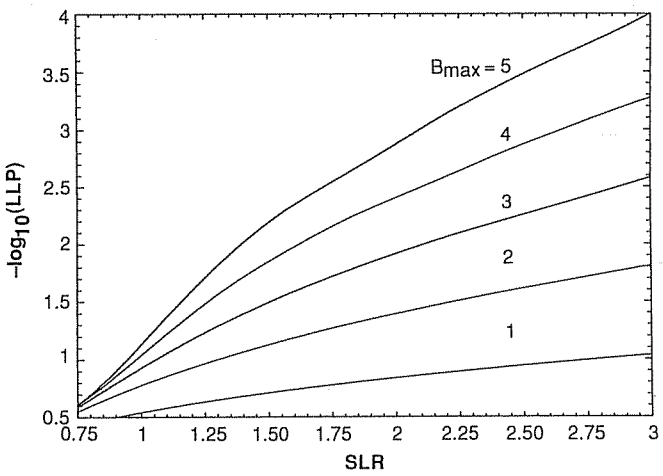

Fig. 6. Loss-of-load probabilities vs SLR for $\phi = 0.30$ and $B_{\max}$ between 1 and 5 for $\overline{K} = 0.3$ ($\sigma_H/\overline{H} = 0.689$).

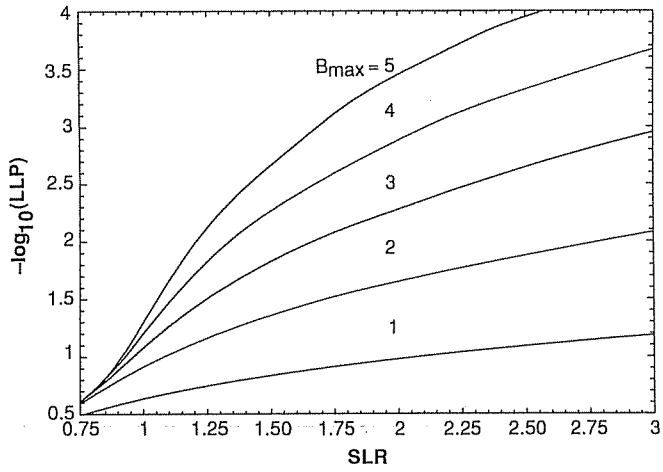

Fig. 7. Loss-of-load probabilities vs SLR for $\phi = 0.30$ and $B_{\max}$ between 1 and 5 for $\overline{K} = 0.4$ ($\sigma_H/\overline{H} = 0.550$).

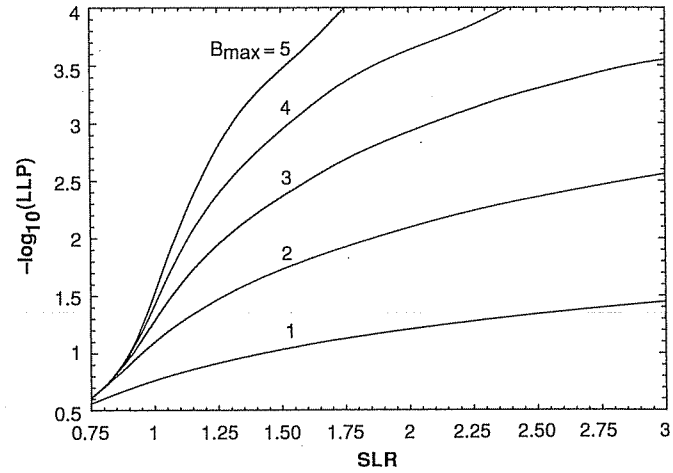

Fig. 8. Loss-of-load probabilities vs SLR for $\phi = 0.30$ and $B_{\max}$ between 1 and 5 for $\overline{K} = 0.5$ ($\sigma_H/\overline{H} = 0.418$).

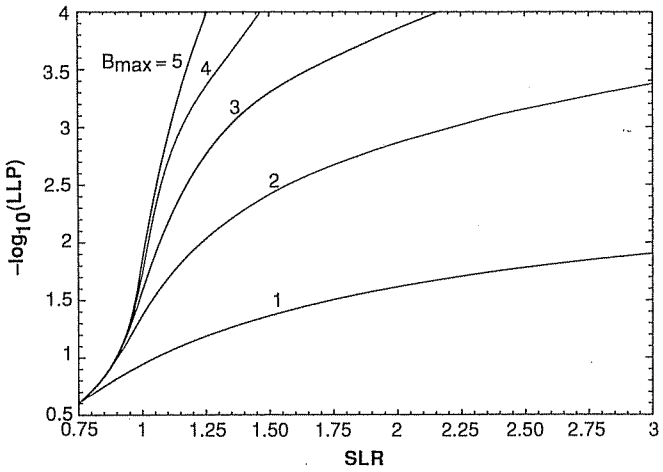

Fig. 9. Loss-of-load probabilities vs SLR for $\phi = 0.30$ and $B_{\max}$ between 1 and 5 for $\overline{K} = 0.6$ ($\sigma_H/\overline{H} = 0.290$).

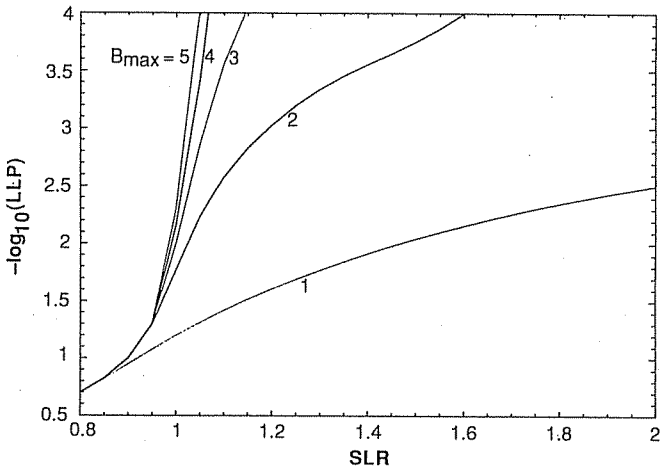

Fig. 10. Loss-of load probabilities vs SLR for $\phi = 0.30$ and $B_{\max}$ between 1 and 5 for $\overline{K} = 0.7$ ($\sigma_H/\overline{H} = 0.165$).

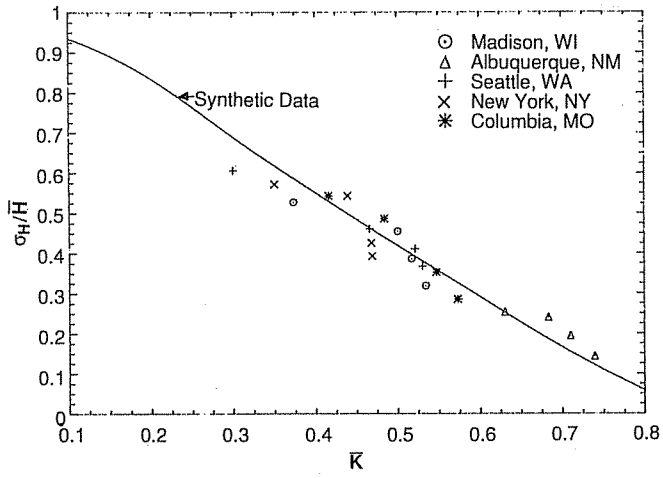

Fig. 11. Relationship between $\sigma_H/\overline{H}$ and $\overline{K}$.

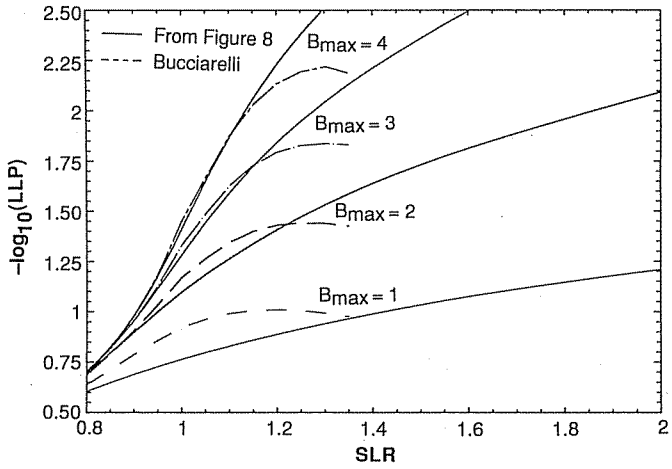

Fig. 12. Comparison of loss-of-load probabilities calculated using Bucciarelli's method[16] with results from Fig. 8.

a sequence of below-average days of radiation that deplete the battery. LLP values are lowest for high values of $\overline{K}$ (e.g., 0.7) since in this case, there is relatively little variability in the daily solar radiation as nearly every day is sunny. Variability increases as $\overline{K}$ decreases down to $\overline{K}$ of about 0.2. Very low values of $\overline{K}$ (e.g., 0.1) again exhibit less variability since, in order to have an average of 0.1, every day tends to be overcast with rare sunny days.

The analytic models of Bucciarelli and Gordon require as an input parameter, σ_a, the standard deviation of the daily array output. It is this parameter that contains information concerning the distribution of the solar radiation. Assuming the load and system efficiency to be constant, σ_a can be related to σ_H, the standard deviation of the daily radiation by

$$\sigma_a = \left(\frac{\text{SLR}}{\overline{H}}\right)\sigma_H \tag{5}$$

The ratio of σ_H to $\overline{H}$ has been found to be a nearly linear function of $\overline{K}$, independent of ϕ, as shown in Fig. 11. The solid line was obtained using the synthetic radiation data. The symbols represent monthly-average values calculated from the 23 and 1/2 year SOLMET data base.

With Fig. 11, a direct comparison can be made between the analytic models and the information in Figs. 4 to 10. Shown in Fig. 12 is a comparison of loss-of-load probabilities calculated using Bucciarelli's model (dotted lines) for $\overline{K} = 0.5$ and $\phi = 0.3$ with those from Fig. 8 (solid lines). (Bucciarelli's loss-of-load probability, Π_E, must be multiplied by his Δ to yield the loss-of-load probability as defined in this study.) Comparisons are shown for $B_{\max}$ (Bucciarelli's C/L) equal to 1 through 4 and good agreement is noted for $B_{\max}$ greater than 1 and for SLR less than about 1.1. Since Bucciarelli's method apparently assumes a uniform 24-hour load distribution, and our results are for a nighttime load, however, his results for a given value of $B_{\max}$ should be compared with ours for $B_{\max} + 1$. Bucciarelli does not mention that his analytic method yields a maximum value of LLP for SLR of about 1.2; increasing SLR beyond this point results in lower values of LLP, contrary to our results and to intuition. Gordon's method also displays this behavior.

6. EFFECTS OF ARRAY ORIENTATION

All of the results presented thus far have been generated assuming the array to be horizontal. Tilting the array has two effects. First, depending on the orientation and time of the year, the average daily radiation on the array plane may be less or greater than the horizontal value, which changes the value of SLR. Long-term averages of the daily solar radiation incident on surfaces with orientations other than horizontal are not generally available and they must thus be estimated from horizontal data. The estimation process requires information concerning the amount of diffuse radiation and its distribution over the sky dome, which has been the subject of many studies (e.g., [20–22]). Klein and Theilacker[23] present an algorithm for estimating $\overline{R}$, the ratio of monthly average radiation on a tilted surface to that on a horizontal surface, assuming diffuse radiation to be isotropic. For surfaces facing directly toward the equator, the isotropic assumption provides conservative (i.e., $\overline{R}$ closer to unity) radiation estimates. Herzog[24] presents a modification to this algorithm to allow for an anisotropic radiation distribution.

A second effect of array orientation is that it alters the distribution of daily solar radiation. This is illustrated in Fig. 13, which shows daily distributions of horizontal radiation for $\overline{K} = 0.3$, 0.4, and

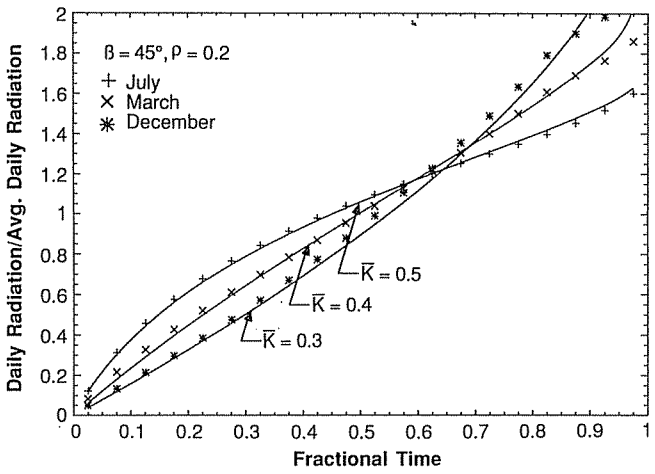

Fig. 13. Comparison of cumulative frequency distributions of daily radiation on a 45° surface at 45°N latitude in March, July, and December with distributions for a horizontal surface.

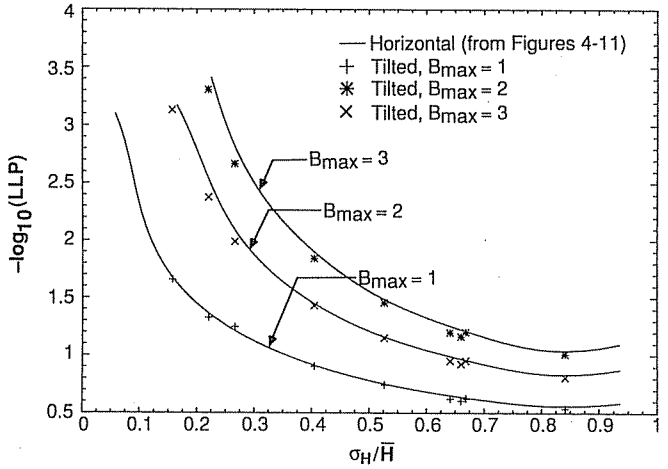

Fig. 14. Relationship of LLP to $\sigma_H/\overline{H}$ for horizontal and tilted surfaces.

0.5 (solid lines) and of the radiation on a 45° south-facing surface at 45°N latitude with $\overline{K} = 0.5$ for March ($\overline{R} = 1.25$), July ($\overline{R} = 0.85$), and December ($\overline{R} = 2.09$), calculated with a ground reflectance of 0.2 and the isotropic diffuse assumption. The distribution for the 45° surface in July closely resembles that for a horizontal surface with $\overline{K} = 0.5$, whereas the distributions for March and December show greater variability and more closely resemble distributions for horizontal surfaces with $\overline{K} = 0.4$ and 0.3, respectively. The general conclusion is that any change (i.e., orientation, time of year, ground reflectance, etc.) that increases $\overline{R}$ also increases the variability of the daily solar radiation, and conversely.

In terms of its effect on LLP, the distribution of daily solar radiation on horizontal or tilted surfaces is described by a single parameter, $\sigma_H/\overline{H}$, the ratio of the daily standard deviation to the long-term average solar radiation on the array surface. This is the parameter plotted against $\overline{K}$ in Fig. 11 for horizontal surfaces. A method of estimating $\sigma_H/\overline{H}$ for other orientations is discussed in the Appendix. The effect of this parameter can be seen in Fig. 14 in which LLP for SLR = 1.2 is plotted against $\sigma_H/\overline{H}$ for $B_{\max}$ values between 1 and 3. The solid lines in this figure correspond to simulation results for horizontal surfaces taken from Figs. 4 through 10. The symbols correspond to results obtained for tilted surfaces for a range of (south facing) orientations, months, and ground reflectances. For the same values of SLR and $B_{\max}$ (and with $\phi = 0.3$), the loss-of-load probability depends only on $\sigma_H/\overline{H}$. Thus Figs. 4 to 10, generated with horizontal data, are equally applicable to other orientations with the same value of $\sigma_H/\overline{H}$. When the array is not horizontal, an appropriate value of $\overline{K}$ corresponding to $\sigma_H/\overline{H}$ is found from Fig. 11 and LLP is read (or interpolated) from Figs. 4 to 10 corresponding to this value of $\overline{K}$.

7. DISCUSSION

Figures 4 to 10 provide an estimate of the auxiliary fraction expected from a system with a given SLR and B_{max} over the long term. However, the system may not necessarily achieve this auxiliary fraction during its lifetime of, say 10 years, because of the variability associated with the estimate. As noted in Section 5, as many as 30,000 days (the equivalent of 1000 years of data for a specified month) may be needed to obtain results that no longer depend on the random number seed value, suggesting that there can be a great deal of variability associated with 10-year (300 day) average auxiliary fractions. This indeed is the case for small auxiliary fractions as seen in Fig. 15 where the distribution of 10-year averages of the auxiliary fraction divided by the long-term average auxiliary fraction (i.e., the LLP) are shown for LLP values of .1, .01, and .001. If the auxiliary fraction for every 10-year period were equal to the LLP, the curves in Fig. 15 would be horizontal lines at an ordinate value of 1.0. This is nearly true for auxiliary fractions greater than .1. As LLP decreases below .1, however, increased variability in the 10 year average auxiliary fractions is observed. When LLP is .001, there is a 50% probability that, during any 10-year period, the system will always supply 100% its load. On the other hand, there is a significant probability that the 10-year average auxiliary fraction will be as much as an order of magnitude larger than intended, as a result of the variability in the solar radiation. For this reason, LLP values less than .01 cannot be considered realistic performance estimates of a system during its lifetime.

7.1 *Example*

Estimate the photovoltaic array area needed to obtain a loss-of-load probability of .05 in Madison, WI (lat. 43°N) during January in supplying a constant nighttime load of 1 kW hr/day. The array is tilted at a 45° angle, facing due south. The overall system efficiency is 0.08.

It is first necessary to estimate $\overline{H}$ and σ_H. The monthly average daily radiation on horizontal surface in January and associated clearness index are 5847 kJ/m^2 day and 0.45, respectively[26]. $\overline{R}$, the ratio of monthly average radiation on the 45° surface to that on the horizontal surface, is estimated using the method of Klein and Theilacker[23] to be 1.70, assuming a ground reflectance of 0.2 and a diffuse fraction of 0.48 as obtained from the correlation of Erbs et al.[20]. $\overline{H}$ is then $1.70 \times 5847 = 9940$ kJ/day. The ratio, $\sigma_H/\overline{H}$ is estimated as described in the Appendix using the Hollands–Huget[3] cumulative distribution curve. With 10, 20, 40, and 80 bins, the values of $\sigma_H/\overline{H}$ are 0.646, 0.672, 0.685, and 0.692, respectively.

From Fig. 11 with $\sigma_H/\overline{H} = 0.69$, the distribution of radiation on the 45° surface in January is equivalent to that on a horizontal surface for $\overline{K} = 0.3$. The relation between LLP, SLR, and B_{max} is thus read from Fig. 6. For LLP = .05 ($-\log 10(\text{LLP}) = 1.30$), the values of SLR are 1.82, 1.32, 1.15, and 1.07 for B_{max} equal to 2, 3, 4, and 5, respectively. (A LLP of .05 can not be obtained with SLR < 3.0 when $B_{max} = 1$.) From eqn (3), the corresponding array areas are 8.2, 6.0, 5.2, and 4.8 m^2.

NOMENCLATURE

- A photovoltaic array area
- AUX fraction of the load not supplied by the solar energy system
- B_d ratio of the useful energy in the battery to the average daily load at the end of the daytime period
- B_n ratio of the useful energy in the battery to the average daily load at the end of the nighttime period
- B_{max} ratio of the maximum useful energy in the battery to average daily load
- DF_j ratio of the daily diffuse to global radiation corresponding to a daily clearness index of K_j

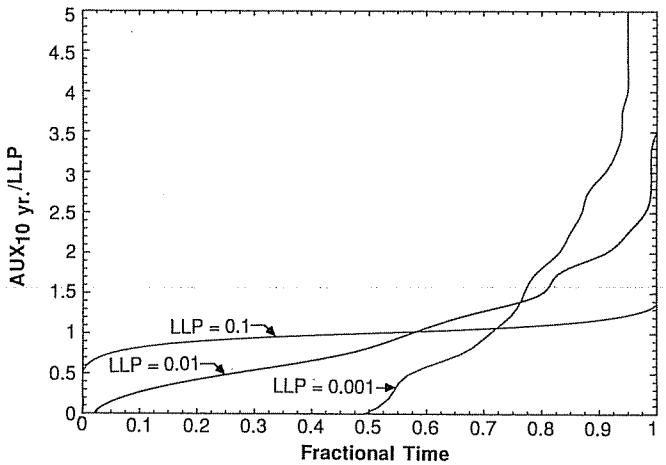

Fig. 15. Distribution of 10-year (300-day) average auxiliary fractions for LLP values of .1, .01 and .001.

f_j fractional time that the daily clearness index is less than K_j
H daily radiation per unit area on the plane of the array
$\bar{H}$ long-term monthly average daily radiation per unit area on the plane of the array
K daily clearness index defined as the ratio of the daily total radiation per unit area on a horizontal surface to the daily extraterrestrial radiation (commonly called K_T)
$\bar{K}$ long-term monthly average value of K
K_{min} minimum value of K
K_{max} maximum value of K
L effective daily electrical load (i.e., the daily load divided by the inverter efficiency, if used)
LLP loss-of-load probability defined as the long-term average value of AUX
$\bar{R}$ ratio of monthly average radiation on an inclined surface to that on a horizontal surface
R_j the ratio of daily radiation on an inclined surface to that on a horizontal surface for a clearness index of K_j
R_b ratio of daily beam radiation on an inclined surface to that on a horizontal surface
SLR solar to load ratio defined by eqn (3)
β tilt of array from horizontal
η photovoltaic system efficiency including charge and discharge efficiencies of the battery
ϕ correlation coefficient between the daily solar radiation on successive days
ρ ground reflectance
σ_a standard deviation of daily array output
σ_H standard deviation of daily radiation per unit area
σ_K standard deviation of daily clearness index values
$\sigma_{\bar{K}}$ standard deviation of monthly clearness index values
σ_ϕ standard deviation of monthly value of ϕ

REFERENCES

1. B. Y. H. Liu and R. C. Jordan, The interrelationships and characteristic distribution of direct, diffuse and total radiation. *Solar Energy* **4**(3), 1–19 (1960).
2. P. Bendt, M. Collares-Pereira and A. Rabl, The frequency distribution of daily insolation values. *Solar Energy* **27**, 1–5 (1981).
3. K. G. T. Hollands and R. G. Huget, A probability density function for the clearness index, with applications. *Solar Energy* **30**(3), 195–209 (1983).
4. S. A. Klein and W. A. Beckman, Review of solar radiation utilizability. *ASME Journal of Solar Energy Engineering* **106**, 393–402 (1984).
5. D. L. Evans, W. A. Facinelli and L. P. Koehler, Simulation and simplified design studies of photovoltaic systems. SAND 80-7013, Sandia Laboratory, Albuquerque, NM (1980).
6. M. D. Siegel, S. A. Klein and W. A. Beckman, A simplified method for estimating the monthly-average performance of photovoltaic systems. *Solar Energy* **26**, 413 (1981).
7. D. R. Clark, S. A. Klein and W. A. Beckman, A method for estimating the performance of photovoltaic systems. *Solar Energy* **33**(6), 551–555 (1984).
8. D. Fox, Y. Zarmi and P. Zoglin, Stochastic model for the long-term behavior of battery storage in photovoltaic systems. *Proc. ISES World Congress*, Montreal, Canada (June 1985).
9. B. Bartoli, V. Cuomo, F. Fontana, C. Serio and V. Silverstrini, The design of photovoltaic plants: An optimization procedure. *Applied Energy* **18**, 37–47 (1984).
10. S. A. Klein, A design procedure for solar heating systems. Doctoral disssertation, Department of Chemical Engineering, University of Wisconsin-Madison (1976).
11. B. J. Brinkworth, Autocorrelation and stochastic modelling of insolation sequences. *Solar Energy* **19**, 343–347 (1977).
12. B. Bartoli, B. Coluaai, V. Cuomo, M. Francesca and C. Serio, Autocorrelation of daily global solar radiation. *Nuovo Cimento* **4C**(2), 113–122 (1981).
13. V. A. Grahm, K. G. T. Hollands and T. E. Unny, Stochastic modeling of the daily solar atmospheric transmittance, Kt. *Proc. ISES World Congress*. Montreal, Canada, 2473–2477 (June 1985); V. Graham, Stochastic synthesis of the solar atmospheric transmittance. Ph.D. Doctoral dissertation, University of Waterloo, Waterloo, Ontario (1985).
14. SOLMET, Hourly solar radiation surface meteorological observations. U.S. National Climatic Center, Asheville, N.C., Vols. 1 and 2 (1978).
15. L. L. Bucciarelli, Jr., Estimating loss-of-power probabilities of stand-alone photovoltaic solar energy systems. *Solar Energy* **32**, 205–209 (1984).
16. L. L. Bucciarelli, Jr., The effect of day-to-day correlation in solar radiation on the probability of loss-of-power in a stand-alone photovoltaic energy system. *Solar Energy* **36**(1), 11–14 (1986).
17. R. N. Chapman, Design consideration for stand-alone photovoltaic systems. *Proc. Symposium on Applications of Solar and Renewable Energy—86*, Cairo, Egypt (March 1986).
18. J. M. Gordon, Stand-alone photovoltaic systems: A stochastic analytic model for predicting loss-of-load. *Proc. ASES Annual Meeting*, Boulder, CO, 373–375 (1986).
19. G. Ambrosone, S. Catalanotti, U. Coscia and G. Troise, Comparison between power and energy methods of photovoltaic plants. *Solar Energy* **34**(1), 1–8 (1985).
20. D. G. Erbs, S. A. Klein and J. A. Duffie, Estimation of the diffuse radiation fraction for hourly, daily, and monthly average global radiation. *Solar Energy* **28**, 293–302 (1982).
21. J. E. Hay, Calculation of monthly mean solar radiation for horizontal and inclined surfaces. *Solar Energy* **23**, 301–307 (1979).
22. R. Perez, R. Stewart, C. Arbogast, R. Seals and J. Scoot, An isotropic hourly diffuse radiation model for sloping surfaces: Description, performance, validation, site dependency evaluation. *Solar Energy* **36**(6), 481–497 (1986).
23. S. A. Klein and J. C. Theilacker, An algorithm for calculating monthly-average radiation on inclined surfaces. *ASME Journal of Solar Energy Engineering* **103**, 29–33 (1981).
24. M. E. Herzog, Estimation of hourly and monthly average daily insolation on tilted surfaces. M.S. thesis in Applied Solar Energy, Trinity University, Trinity, TX (1985).
25. P. R. Armstrong, How weather persistence affects performance of solar heating systems. M.S. thesis in Mechanical Engineering, Colorado State University, Fort Collins, CO (1980).
26. J. A. Duffie and W. A. Beckman, *Solar Engineering of Thermal Processes*. Wiley Interscience, New York, 90–95 (198x).

APPENDIX

Estimation of $\sigma_H/\overline{H}$

Ideally, both $\overline{H}$ and $\sigma_H/\overline{H}$ would be determined from historical records of daily radiation for the location and surface orientation of interest. Unfortunately, long-term records of daily solar radiation are rarely available on tilted surfaces and so these quantities will usually have to be estimated based on long-term monthly average horizontal radiation data. $\overline{H}$ can be estimated as described in [23]. A simple means of estimating $\sigma_H/\overline{H}$ follows.

Given the value of $\overline{K}$, the fractional time that the daily clearness index, K, is less than a specified value can be obtained from the cumulative distributions of Liu and Jordan[1], Bendt et al.[2], or Hollands and Huget[3]. To estimate $\sigma_H/\overline{H}$, divide the K axis into a number (e.g., 20) of equally sized bins. R_j, the ratio of the radiation on the tilted surface to that on a horizontal surface for bin j is calculated as a function of K_j, the K value at the center of the bin. Assuming isotropic diffuse and ground reflected radiation, R_j is approximately given by

$$R_j = \frac{(1 - DF_j)R_b + DF_j(1 + \cos\beta)}{2} + \frac{\rho(1 - \cos\beta)}{2} \quad \text{(A.1)}$$

where

R_b is the ratio of daily beam radiation on the tilted surface to that on the horizontal surface. An equation for R_b that assumes a constant atmospheric transmittance is given by Duffie and Beckman[26]. A somewhat more complicated equation that considers the diurnal variation of the atmospheric transmittance is given by Klein and Theilacker[23].

β is the slope of the surface from horizontal

ρ is the ground reflectance

DF_j is the ratio of daily diffuse to global radiation that can be estimated from a correlation established by Erbs et al.[20] in terms of K_j

$$DF_j = \begin{cases} 1.00 + 0.235K_j - 2.258K_j^2 - 1.760K_j^3 & \text{for } K_j > 0.72 \\ 0.165 & \text{for } K_j >= 0.72 \end{cases} \quad \text{(A.2)}$$

After computing R_j for all bins, the value of $\sigma_H/\overline{H}$ can be calculated from

$$\sigma_H/\overline{H} = \frac{\sqrt{\sum[(f_j - f_{j-1})\,(K_jR_j - \overline{KR})^2]}}{\sum[(f_j - f_{j-1})R_jK_j]} \quad \text{(A.3)}$$

where

f_j is the fractional time corresponding to K_j from the cumulative distribution curves and f_0 is 0.

and

$$\overline{KR} = \sum[(f_j - f_{j-1})R_jK_j] \quad \text{(A.4)}$$

The value of $\sigma_H/\overline{H}$ obtained from eqn A.3 is only slightly affected by choosing more than 10 bins in the calculation (as seen in the Example) or by other factors such as the ground reflectance and the consideration of diurnal variation of atmospheric transmittance. $\sigma_H/\overline{H}$ will probably show little sensitivity to assumptions made regarding the distribution of diffuse radiation (i.e., isotropic or anisotropic) but this was not tested. On the other hand, more than 50 bins are needed to obtain accurate estimates of $\overline{R}$ with eqn A.4. For consistency, the product $\overline{KR}$ in eqn A.3 should be obtained with eqn A.4.